LA-UR-01-4789
Approved for public release; distribution is unlimited.

Title: **Measurements of Neutron Spectra in 0.8-GeV and 1.6-GeV Proton-Irradiated W and Na Thick Targets**

Author(s): Yury E. Titarenko, Vyacheslav F. Batyaev, Evgeny I. Karpikhin, Valery M. Zhivun, Alexsander B. Koldobsky, Ruslan D. Mulambetov, Dmitry V. Fischenko, Svetlana V. Kvasova, Yury V. Trebukhovsky, Vladmir A. Korolev, Gennady N. Smirnov, Stepan G. Mashnik, Richard E. Prael, Arnold J. Sierk, Hideshi Yasuda

Submitted to:

http://lib-www.lanl.gov/la-pubs/00818513.pdf

MEASUREMENTS OF NEUTRON SPECTRA IN 0.8-GEV AND 1.6-GEV PROTON-IRRADIATED W AND NA THICK TARGETS

Yury E. Titarenko, Vyacheslav F. Batyaev, Evgeny I. Karpikhin, Valery M. Zhivun,
Aleksander B. Koldobsky, Ruslan D. Mulambetov, Dmitry V. Fischenko,
Svetlana V. Kvasova, Yury V. Trebukhovsky, Vladimir A. Korolev, Gennady N. Smirnov
Institute for Theoretical and Experimental Physics, B.Cheremushkinskaya 25,
117259 Moscow, Russia, e-mail: Yury.Titarenko@itep.ru
Stepan G. Mashnik, Richard E. Prael, Arnold J. Sierk
Los Alamos National Laboratory, Los Alamos, NM 87545, USA
Hideshi Yasuda
Japan Atomic Energy Research Institute, Tokai, Ibaraki, 319-1195, Japan

August 10, 2001

ABSTRACT

Measurements of neutron spectra in W, and Na targets irradiated by 0.8 GeV and 1.6 GeV protons are presented. Measurements were made by the TOF techniques using the proton beam from the ITEP U-10 synchrotron. Neutrons were detected with BICRON-511 liquid scintillator-based detectors. The neutron detection efficiency was calculated via the SCINFUL and CECIL codes.

The W results are compared with the similar data obtained elsewhere. The measured neutron spectra are compared with the LAHET and CEM2k code simulation results. Attempt is made to explain some observed disagreements between experiments and simulations.

The presented results are of interest both in terms of nuclear data buildup and as a benchmark of the up-to-date predictive power of the simulation codes used in designing the hybrid accelerator-driven system (ADS) facilities with sodium-cooled tungsten targets[1, 2].

FOREWORD

The data on the neutrons and charged particles generated in proton beam interaction with target and structure materials are unavoidable when designing the present-day ADS facilities with 1-2 GeV proton beam energies. The data accuracy requirements are rather strict because the data determine the external source term of the ADS. Besides, the neutron and proton data determine the calculation accuracy requirements of such principal ADS blanket parameters as k_{eff}, safety control system efficiency, energy deposition of the fuel assembly, and minor actinide transmutation rates. The data are also important in calculating the radiation resistance of structure materials exposed to high-energy particles.

Tungsten belongs to the most promising materials for the multiplying targets of ADS facilities. Tungsten is sufficiently feasible technologically, shows the necessary set of nuclear-physics characteristics, and is devoid of any chemical reactivity and biological toxicity (as contrasted with, for example, lead and mercury). It should also be allowed for that the actual target designs involve not only the neutron generators made of heavy materials, but also the cooling and heat-exchanging units. Sodium is often regarded as a promising material for those units, considering that the sodium-based technologies have been studied in sufficient detail and mastered in designing and operating fast breeders.

In view of the above, the problem arises as to accumulating and estimating the microscopic and group nuclear constants for the above-mentioned materials and their associate assemblies. Meanwhile, the experiments with measuring the constants in the case of tungsten and nickel are still scanty to meet the actual requirements of designing and servicing the ADS facility targets. According to the review [3], for instance, the measurements of the double differential spectra of secondary neutrons outgoing from a proton-irradiated tungsten target are described in but three works [4, 5, 6]. Any relevant sodium data are absent at all. It is very urgent, therefore, to experiment with the space-energy characteristics of secondary neutrons from the tungsten and sodium targets irradiated by intermediate- and high-energy protons.

The group of the Institute of Theoretical and Experimental Physics (ITEP) measured the neutron spectra in 0.8 GeV and 1.6 GeV proton- irradiated thick tar-

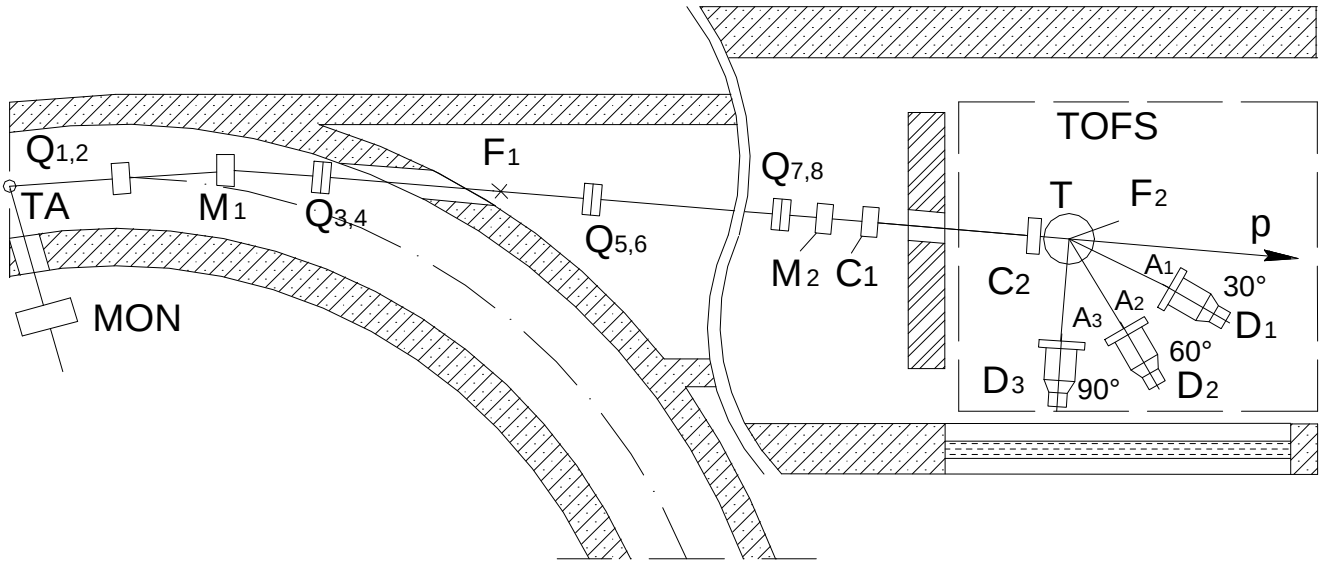

Figure 1: The key diagram of the mutual arrangement of the proton beam elements and the TOF spectrometer. TA is the ITEP synchrotron inner target. MON is the beam monitor. $Q_{1,2}$ – $Q_{7,8}$ are the quadrupole magneto-optic lenses. M_1 and M_2 are the bending magnets. F_1 and F_2 are the first and second focus of the beam. C_1 and C_2 are the proton detectors (0.5-1.0-cm thick plastic scintillators) that are spaced 12m apart and constitute the beam telescope. D_1 – D_3 are the detecting stacks composed each of a neutron detector and its anticoincider. The inner and experimental targets are spaced ~80 m apart.

gets via W(p,xn) and Na(p,xn) reactions. The measurements were made by the time-of-flight (TOF) techniques; the neutron yields were measured at angles of 30^o, 60^o, 90^o, 120^o, and 150^o in the laboratory frame of reference. The measurement results were compared with the simulation data obtained by the LAHET code system [13] and CEM2k code [14].

The tungsten results have been compared with the like data obtained in [6].

EXPERIMENTAL DESIGN

The experiment was made using the time-of-flight spectrometer (TOFS) located in the 512-th beam of the ITEP proton synchrotron with a 10 GeV maximum energy (see Fig. 1).

The charged particles, which are ejected at 3.5^o in the accelerated proton interactions with the nuclei of inner Be foil target, get focused to the intermediate focus F_1 by the magnetic dipole M_1 and by the quadrupoles $Q_{1,2}$ and $Q_{3,4}$ and, after that, to the focus F_2 (wherein the target center is located) by the magnetic dipole M_2 and by the quadrupoles $Q_{5,6}$ and $Q_{7,8}$. The operations with a pure proton beam at given energies of secondary protons were attained to by tuning the secondary beam outfit to the quasielastic peak of protons scattered from the inner target. The FWHM dimension of the beam is 18x24 mm at focus F_2. The secondary beam pulse duration on the target is 0.8 s. The performance mode of up-to 10^5 protons per a pulse was used to attain the optimal spectral measurements of the particles outgoing from the targets. The low intensity and the long proton pulse duration of the beam selected in the experiment have made it possible to separately record each of the measurement parameters for the appropriate particles. The protons incident onto a target were recorded with a telescope of two thin scintillators C_1 and C_2. Neutrons were recorded with the detecting stacks D_1 - D_3 that consist each of a neutron detector (D12.7x15.2cm BICRON MAB-511 liquid scintillator) and a 2-cm thick NE102A plastic scintillator placed before the latter. The NE102A anticoincidence operation mode turns the scintillator into a veto detector to exclude the charged particles that move towards the neutron detector. The detectors were placed at more than 5m from the ceiling and walls of the room, and at 2.5m from its floor. The neutron detectors operated without any additional shielding because the preparatory measurements and calculations have shown but an insignificant contribution from the scattered neutron background. During the measurement runs, the detectors were placed at angles of 30^o, 60^o, 90^o or 90^o, 120^o, 150^o to the proton beam axis.

The TOF logic of the spectrometer is as follows. The measuring circuit is triggered by a coincidence event between a beam telescope pulse and a pulse from one of the neutron detectors. The neutron TOF metering circuit is triggered by a pulse from one of the neutron detectors, while the stop pulse is a C_2 detector pulse.

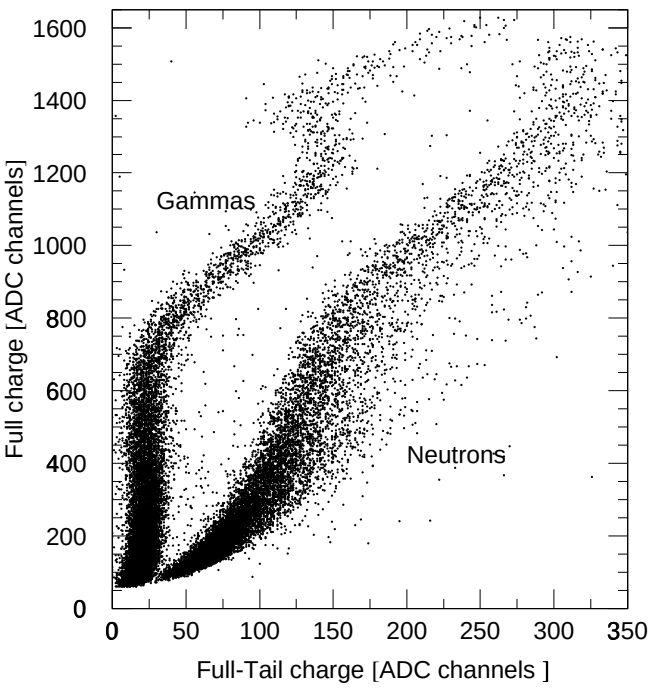

Figure 2: Neutron-gamma separation by the amplitude-amplitude analysis

This time inversion procedure has simplified the measurement logic pattern. The probability for an event to be recorded by two detectors simultaneously is very low (below 1%), so but a single time measurement circuit was used. The circuit converts the time interval between the trigger and stop pulses into a charge labeled a digit to designate number of a given channel. The same procedure was used to record some parameters that are necessary for neutrons and gammas to be separated by their pulse shapes in a detector.

The information about each of the detected events was computer- memorized using the MES [7] code. The memorized primary experimental data processing included the neutron-gamma separation and the calculations of the neutron spectra. The main experimental design data can be found in Table 1.

NEUTRON-GAMMA SEPARATION

Neutrons were separated from gammas by the amplitude-amplitude analysis of a recorded particle pulse (A(total charge) - A(tail charge)) within a 2.5 MeV - $\sim$ 10 MeV recoil proton energy range, and by the amplitude-time (A(total charge)- T(pulse duration)) analysis within s $\sim$ 10 - 300 MeV recoil proton energy range. The former method permits reliable separation of small-amplitude pulses (see Fig. 2). The latter method separates large-amplitude pulses (Fig. 3), for which the quality of the amplitude-amplitude separation is lost.

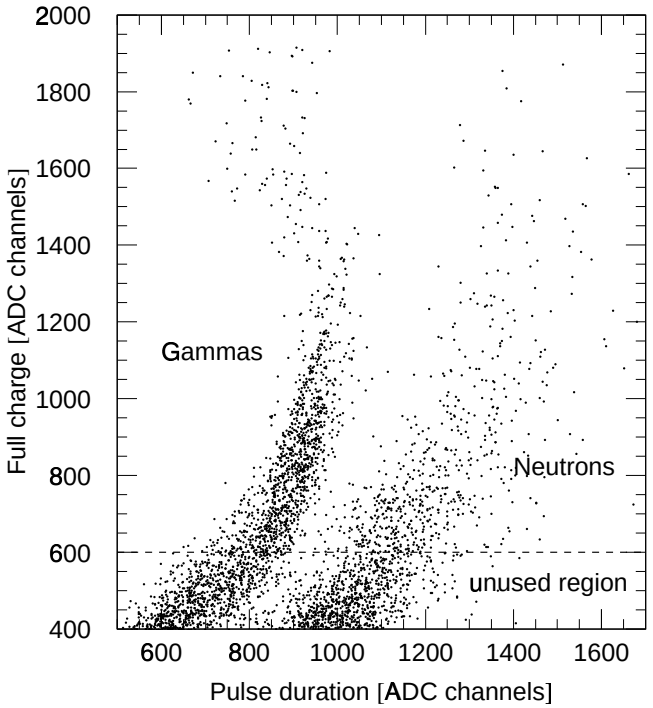

Figure 3: Neutron-gamma separation by the amplitude-time analysis.

The plot in Fig. 3 demonstrates the branch behavior of the amplitude-time separation technique. From the figure it follows that, as the pulse amplitude increases, the branches that correspond to neutrons and gammas diverge and the separation quality rises accordingly. Thus, an acceptable separation quality is achieved by appropriate matching the parameters in the range of small pulse amplitudes, and using the amplitude-time separation technique in the range of large pulse amplitudes.

NEUTRON DETECTION EFFICIENCY

Figs. 6 and 7 show the space-energy distributions of the secondary neutrons outgoing from the targets (in absolute units per an incident proton). The distributions have been obtained using the values of the neutron detection efficiency in the liquid scintillators of the above mentioned dimensions. In their turn, the values were calculated by the SCINFUL ([8], E_n <80 MeV) and CECIL ([9], E_n >80 MeV) codes. The CECIL-calculated values were normalized to reach a smooth fit to the SCINFUL results at 80 MeV. Fig. 4 presents the results of calculating the neutron detection efficiency at the discrimination threshold that correspond to E_γ=661keV (^{137}Cs).

The errors of calculating the detection efficiency was taken to be 10% below 80 MeV and 15% above 80 MeV. The given error levels were recommended [10, 11] for the liquid scintillation neutron counters of the like volume.

Table 1: Experimental design data

Target	Target dimensions [cm]	Target Composition [mass %]	Target Density [g/cm^3]	Detector-target distance [m]	
				0.8 GeV	1.6 GeV
W	D5x2.935	W - 97.5, Ni - 1.75, Fe - 0.75, impurities-< 0.2	18.6	1.5	2.0
Na*	D6X20	Na->99.98, impurities - <0.02	0.97	1.5	1.5

* in three steel containers of 10-cm (1) and 5-cm (2) lengths with 0.4-mm thick front walls and 0.8-mm thick cylindrical side wall.

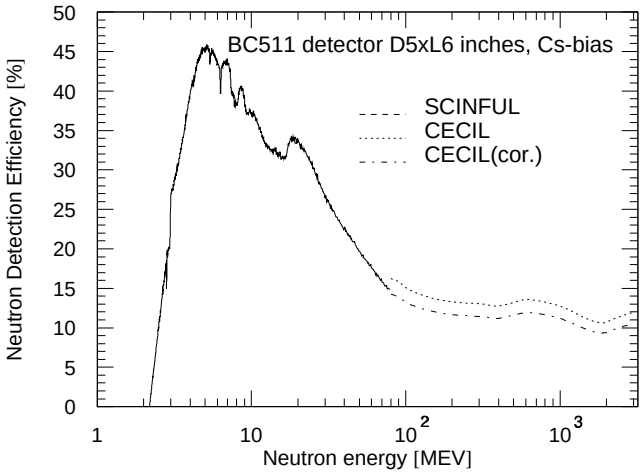

Figure 4: Detection efficiency of the D5xL6 inches BC511 detector used to record neutrons. The calculations are by the SCINFUL and CECIL codes at the threshold corresponding to ^{137}Cs.

ENERGY RESOLUTION OF THE SPECTROMETER

The neutron spectrometer resolution is defined by the following two components that affect the accuracy of determining the velocities (and, hence, energies) of the recorded neutrons.

- The space resolution, which is defined by the dimensions and the mutual arrangement geometry of the target and the counter. Here, the space resolution was taken to be 0.424 ($0.5\sqrt{2ln2}$) of the detector length (target thickness).

- The time resolution, which is defined by the speed of meters, by the photoelectron TOF fluctuations in photomultiplier, and by the light TOF fluctuations in scintillator.

The time resolution was quantitatively estimated by the width of the instantaneous γ-peak of the TOF spectrum in the auxiliary experiment with a "thin" target (2-cm thick lead was used as the latter). The time resolution was found thus to be 0.67 ns. The energy

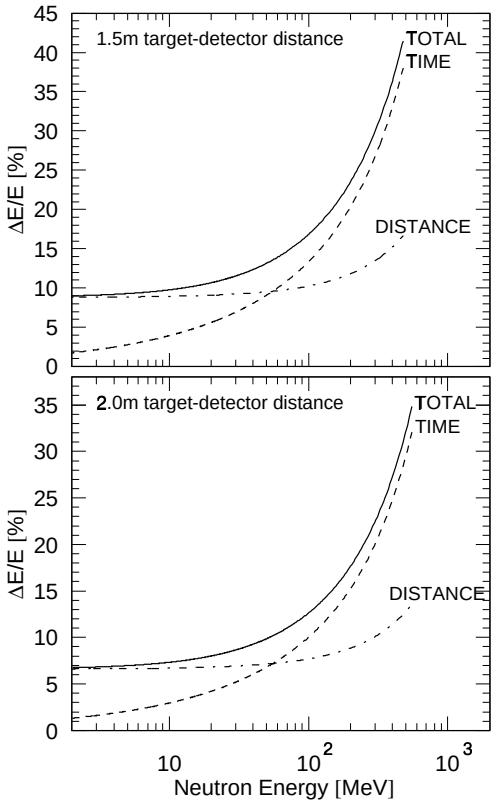

Figure 5: The partial and total values of the energy resolution of the neutron TOF spectrometer, given two TOF bases.

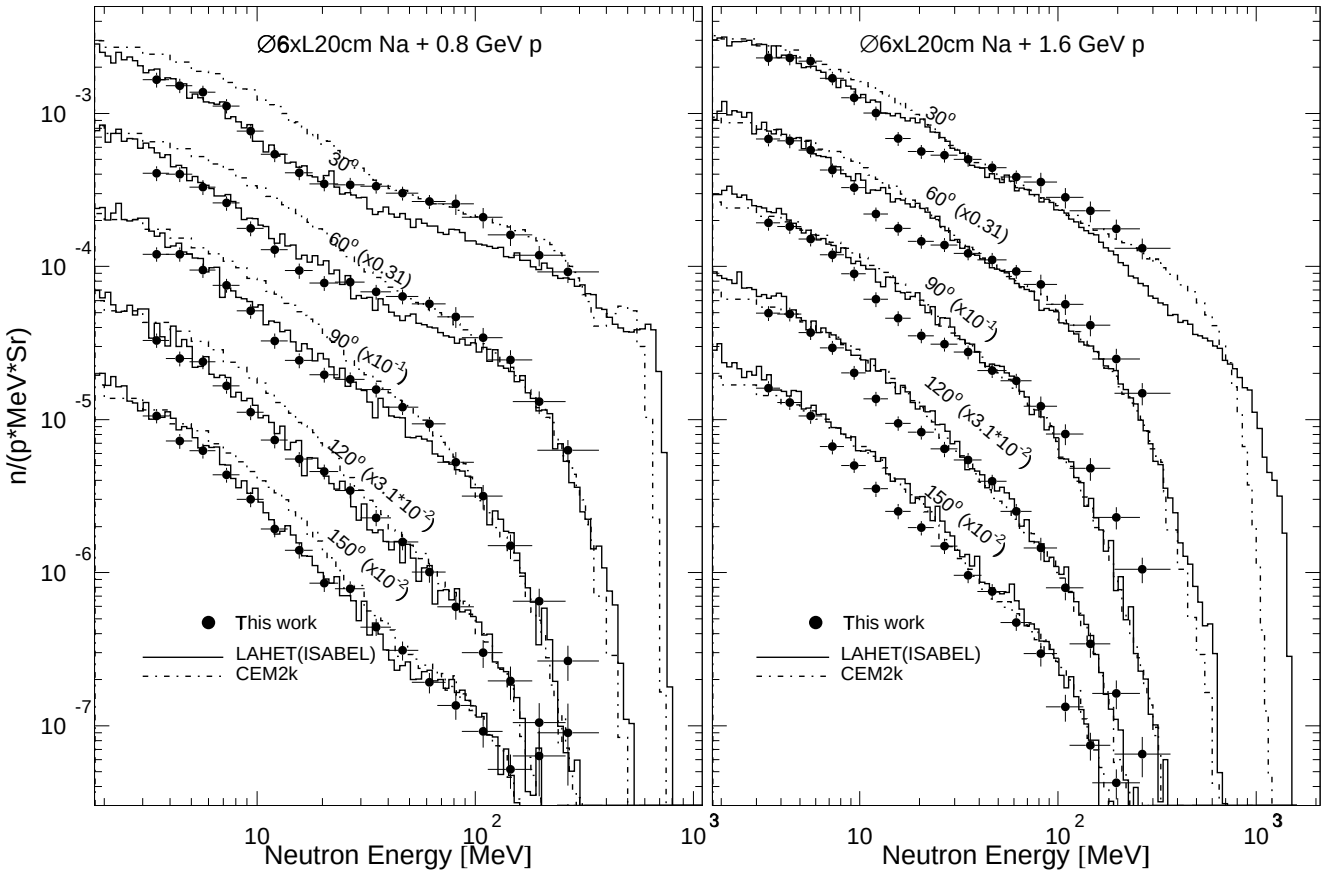

Figure 6: The double differential neutron spectra measured in the present work from D6xL20 cm Na irradiated by the 0.8 (the left-hand panel) and 1.6 (the right-hand panel) GeV protons, together with the LAHET [13] and CEM2k [14] code calculation results.

resolution of the spectrometer (see Fig. 5) was determined by formula (1) using the time (ΔT) and space (ΔL) resolutions that were obtained making allowance for the dimensions of the detectors and targets:

$$\frac{\Delta E}{E} = \gamma(\gamma+1)\sqrt{\left(\frac{\Delta L}{L}\right)^2 + \left(\frac{\Delta T}{T}\right)^2}, \qquad (1)$$

where γ = 1+E/m is the relativistic Lorentz factor.

With the 1.5-m and 2.0-m detector-target spacings, the ultimate neutron energy is respectively 300 MeV and 450 MeV for the energy resolution to be below 30%.

RESULTS

The results obtained are displayed in Figs. 6 and 7. Besides, the experimental data [6] are presented in the case of 0.8 MeV proton-irradiated tungsten. The comparison between the present results and the results of [6] shows that they are in an agreement, especially at neutron energies above 20 MeV. In the range below 20 MeV, the [6] results run, on the average, 20-30% above the present results. The difference is probably due to an uncertainty in the neutron detection efficiency. The fact is that the work [6] made use of another detector type (plastic), whose efficiency was determined experimentally by neutrons from the ^{7}Li(p,n)^{7}Be reaction, rather than via calculations. Therefore, the real reasons for the difference can only be found by experimental testing the detection efficiency of the detectors used in the present work, just as done in [12].

CODE SIMULATION

The experimental data were compared with the results of simulation by the extensively used LAHET [13] (with the ISABEL model) and a preliminary version of the CEM2k [14] codes.

Since the actual experimental targets cannot be regarded as thin, the LAHET simulation of the spectra included the simulation of not only the proton-nucleus interactions, but also the multiple scattering of primary protons and low-energy (below 20 MeV) neutron transport inside the targets by the HMCNP code. The $>$ 20 MeV neutron elastic scattering was allowed for in the case of tungsten.

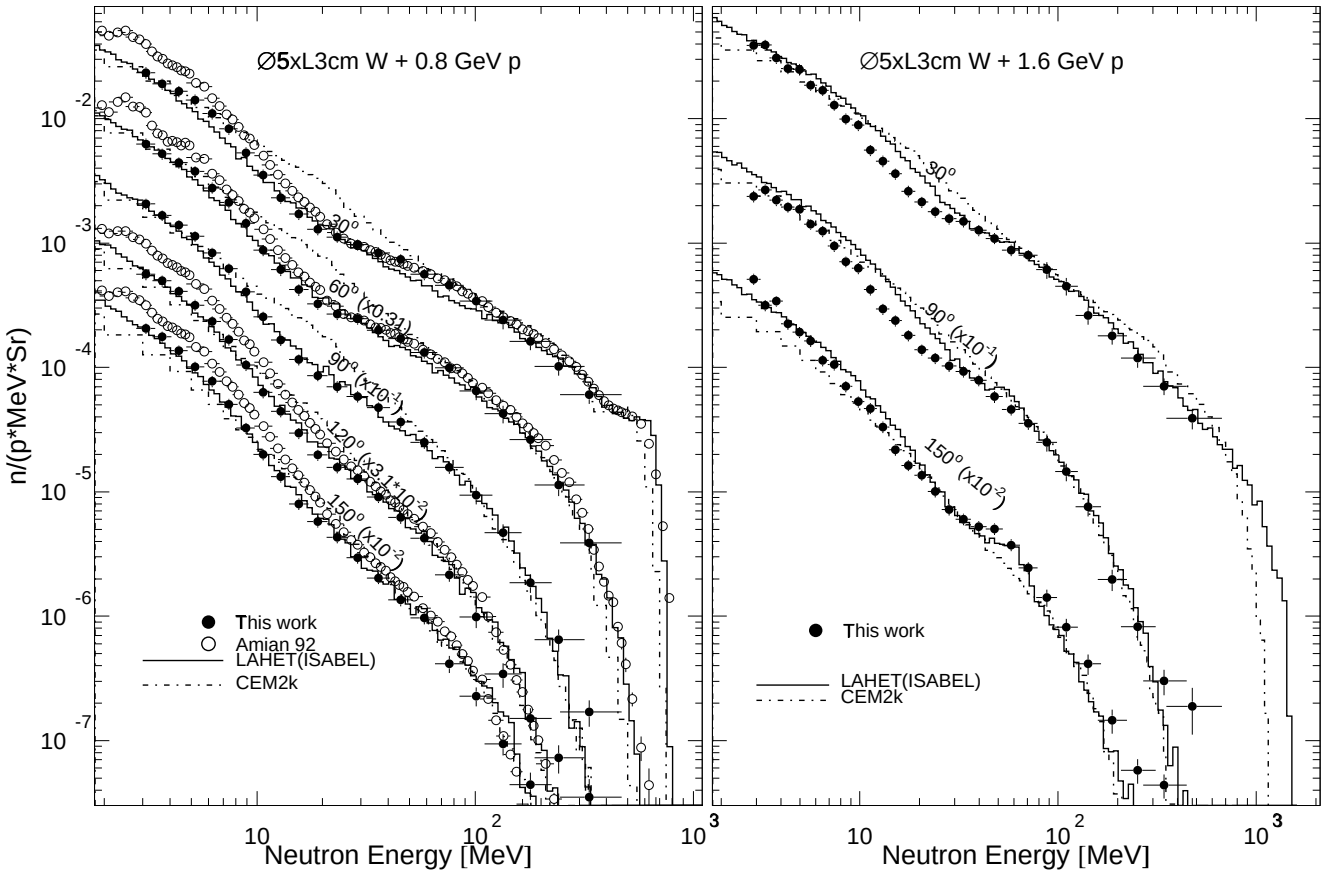

Figure 7: The double differential neutron spectra from D5xL2.935 cm W irradiated by the 0.8 GeV (the left-hand panel) and 1.6 GeV (the right-hand panel) protons, as measured in the present work and in [6] for 0.8 GeV protons, together with the LAHET [13] and CEM2k [14] code calculation results.

The results of calculating the neutron spectra from 0.8 GeV and 1.6 GeV proton-irradiated tungsten and sodium at 30^o, 60^o, 90^o, 120^o, and 150^o are presented in Figs. 6-7 together with the experimental data.

COMPARISON BETWEEN EXPERIMENT AND CALCULATION

The comparison has shown a satisfactory convergence of the LAHET results for tungsten, especially in the case of 0.8 GeV protons. The comparison results indicate that LAHET reproduces properly all the features of the neutron angle-energy distributions throughout the neutron energy range. These results may suggest that our measurement data may be more reliable compared with [6]. At the same time, this conclusion cannot probably be regarded as final and should be supported by the above mentioned auxiliary experiments. The comparison between the experiment and the LAHET results for sodium shows a good agreement at angles 90^o and above but the calculation results are either up to 1.5 times below the experiment in the pre-equilibrium evaporation energy range (E_n=20–200 MeV, E_p=0.8GeV) or up to 2.0 times above in the junction of evaporation and pre-equilibrium energy ranges (E_n=10–30 MeV, E_p=1.6GeV).

The comparison between the experiment and the CEM2k results for tungsten shows a satisfactory agreement in the evaporation (up to 10 MeV) and cascade (above 50 MeV) neutron ranges. At the same time, the neutron yield is overestimated (by a factor of up to 2) in the pre-equilibrium evaporation energy range (10-50 MeV). In the case of sodium, only the neutron yield backwards (150^o) and the cascade neutrons (above 50 MeV) are predicted satisfactorily. The evaporation neutron yield is overestimated by a factor of up to 2, especially in the case of the yields forwards. As a rule, the CEM2k results are in a little worse agreement with experiment compared with LAHET. An explanation may be partly in that, contrary to the LAHET code, CEM2k simulates only the proton-nucleus interactions and does not contain a description of secondary particle transport inside the target (to be used in transport simulations, CEM2k is being incorporated at present into the transport code MCNPX). In addition, CEM2k is

still under development and we used here a preliminary version as described in [14].

As a whole, the convergence of the calculation results is worse in the case of sodium compared with tungsten. The conventional explanation lies in an inadequacy of the current theoretical models used to describe the high-energy hadron interactions with low-mass nuclei. The disagreement of the two codes with the experiment in the case of the cascade neutron yield suggests that the local Fermi distribution of intranuclear nucleons used in both codes should be regarded as a too rough approximation. Both LAHET and CEM2k overestimate the neutron yield in the junction of evaporation and pre-equilibrium energy ranges (E_n=10–30 MeV, E_p=1.6GeV).

ACKNOWLEDGEMENT

The authors are indebted to Dr. S. Meigo (JAERI) for his assistance in calculating the detection efficiency, to Dr. O.A. Shcherbakov (PINP, Gatchina) for helpful discussions of the measurement techniques, to Dr. V.L. Romodanov (MEPI, Moscow) for his presenting the 14 MeV neutron source to be used in detector calibration, to Drs. V.N. Kostromin and I.A. Vorontsov (ITEP, Moscow) for their assistance in carrying out the experiments, and to Dr. F. E. Chukreev (KIAE, Moscow) for discussion of the results.

The work has been carried out under ISTC Project #1145 and supported by JAERI (Japan) and, partly, by the U.S. Department of Energy.

REFERENCES

[1] T. Takizuka et al., "Conceptual Design Study of Accelerator- Driven Systems for Nuclear Waste Transmutation", Proc. of the Second International Conference on Accelerator Driven Transmutation technologies and Applications, June 3-7, 1996, Kalmar, Sweden, pp. 179-185, 210-216.

[2] G. Van Tuyle and D. E. Beller, "Accelerator Transmutation of Waste Technology and Implementation Scenarios", Proc. of the Third International Topical Meeting on Nuclear Applications of Accelerator Technology (AccApp'99), Long Beach, California, November 14-18, 1999, pp.337-346.

[3] Y. Watanabe et al., Status of Experimental Data of Proton Induced Reactions for Intermediate Energy Nuclear Data Evaluation , Proc. of the Third Specialist's Meeting on High Energy Nuclear Data , March 30-31, 1998, JAERI, Tokai, Japan, JAERI-Conf 98-016, 16-29.

[4] M.M. Meier et al., Radiation Effects 96, 73 (1986)

[5] M.M. Meier et al., Nucl. Sci. Eng., 102, 310 (1989)

[6] W.B. Amian et al., Nucl.Sci.Eng., 112, 78 (1992); W.B. Amian et al., Nucl.Sci.Eng., 115, 1 (1993).

[7] N.V. Gorbunov et al., JINR Preprint P-10-85-955, 954 [in Russian].

[8] J.K. Dickens, ORNL-6452, (1988); v. 4, S. Meigo, private communication.

[9] R.A. Cecil et al, Nucl. Instrum. Methods, 161, 439, (1979); v. KSU, S. Meigo, private communication.

[10] K. Ishibashi et al, J. Nucl. Sci Technol., 34, 529 (1997).

[11] T. Nakamoto et al., J. Nucl. Sci Technol., 32, 827 (1995).

[12] S. Meigo, JAERI-Conf-98-016 (Ed. T. Fukahori), 31 (1998).

[13] R.E. Prael, H.Lichtenstein, LANL Report LA-UR-89-3014 (1989).

[14] S. G. Mashnik and A. J. Sierk, "CEM2k - Recent Developments in CEM," in *Proc. of the Fourth International Topical Meeting on Nuclear Applications of Accelerator Technology (AccApp00), November 13-15, 2000, Washington, DC, USA*, (American Nuclear Society, La Grange Park, IL, USA, 2001) pp. 328-341; http://xxx.lanl.gov/ps/nucl-th/001164.